Causal Network in a Deafferented Non-human Primate Brain

Karthikeyan Balasubramanian[1], *Member IEEE-EMBS*, Kazutaka Takahashi[1], *Senior Member IEEE*, Nicholas G Hatsopoulos[1,2]

***Abstract*— De-afferented/efferented neural ensembles can undergo causal changes when interfaced to neuroprosthetic devices. These changes occur via recruitment or isolation of neurons, alterations in functional connectivity within the ensemble and/or changes in the role of neurons, i.e., excitatory/inhibitory. In this work, emergence of a causal network and changes in the dynamics are demonstrated for a deafferented brain region exposed to BMI (brain-machine interface) learning. The BMI was controlling a robot for reach-and-grasp behavior. And, the motor cortical regions used for the BMI were deafferented due to chronic amputation, and ensembles of neurons were decoded for velocity control of the multi-DOF robot. A generalized linear model-framework based Granger causality (GLM-GC) technique was used in estimating the ensemble connectivity. Model selection was based on the AIC (Akaike Information Criterion).**

***Index Terms* - Causality analysis, non-human primates, Brain-machine Interface, Poisson point-process, neural dynamics**

I. INTRODUCTION

Motor cortical regions have polysynaptic innervations to peripheral systems executing motor goals. Chronic amputation causes both motor circuit dysfunction and loss of peripheral actuators, causing de-afferentation and de-efferentation in the brain regions. In such cases, Brain machine interfaces (BMIs) are potential alternatives that can decode neurons towards controlling prosthetic devices through operant conditioning [1]. As BMI learning occurs, the connectivity and information flow within the ensemble of neurons tend to change [2][3] and the motor behavior becomes more volitional and controllable. These observable changes provide information on the network dynamics that can be potentially harnessed to devise robust neuroprosthetic controllers. Anatomical connectivity of network projections are often estimated using axonal tracing [4][5] and other anterograde/retrograde methods in micro and meso scales [6][7][8]. Digital histology and fMRI are being used to understand the large scale architecture in the brain [9]. Nevertheless, they do not lend direct applicability to BMIs. Statistically inferred functional connectivity and causal changes, however, can be used in systematically designing and adapting decoders for improved BMI performance. Changes in a causal network can occur in one of the three known ways, i.e., by including or excluding neurons in an ensemble controlling the BMI, by modifying the strength and directionality and/or by assuming roles of excitation/inhibition.

In this work, network dynamics of an ensemble of motor neurons were observed using a GLM framework based on Granger Causality. We show that as BMI motor learning occurs with a behavioral task, the causal network dynamics undergo changes in terms of recruitment, strength and role of the ensemble elements. We also show that the local-fields also increase their coherencies in the β and the low-γ bands. Spiking activity of neurons were decoded from the motor cortical regions of a non-human primate controlling a multi-DOF robot via a multi-electrode array interface. The region from which the neural signals were acquired was deafferented for several years and hence, the observed network changes are arguably due to the BMI learning.

[1]Karthikeyan Balasubramanian, Kazutaka Takahashi and Nicholas G Hatsopoulos are with the Department of Organismal Biology and Anatomy, University of Chicago, Chicago, IL, USA karthikeyanb@uchicago.edu kazutaka@uchicago.edu

[2]Nicholas G Hatsopoulos is with the Committee on Computational Neuroscience, University of Chicago, Chicago, IL, USA nicho@uchicago.edu

II. EXPERIMENTAL METHODS

A. Implantation and Neural Recordings

A transradially amputated Rhesus macaque (Macaca Mulatta) was chronically implanted with a 100-electrode array in the motor cortical area (M1) estimated to be controlling the arm/hand muscles. A standard multi-electrode array (MEA) (1.0 mm electrode length and 400 μm pitch from Blackrock Microsystems, Inc. Salt Lake City, UT) was used for the implantation. The surgical and behavioral procedures involved in this study were approved by the University of Chicago Institutional Animal Care and Use Committee and conform to the principles outlined in the Guide for the Care and Use of Laboratory Animals.

B. Brain-machine Interface

The animal was operantly conditioned to control a multiple DOF robot, details of which can be found in [10]. The behavioral task comprised generating, (a) reach-dimension velocities to move the robotic arm towards and away from the target object and (b) grasp velocities, controlling the opening and closing of the aperture formed by the three digits of the robotic hand. Two distinct subset of neural units, dubbed as reach and grasp clusters, controlled the reach and the grasp dimensions independently. The reach cluster was heuristically formed based on spatial proximity and the grasp cluster was chosen through a multi-resolution connectivity algorithm [11]. A 20-tap static Wiener-filter was used to estimate the control velocity from the binned spikes. An unsupervised decoder [12] initialization technique was used to determine the tap weights. Action potential spikes recorded by the MEA were sorted and binned into 50

978-1-4244-9270-1/15/$31.00 ©2015 IEEE

TABLE I

GRANGER CAUSALITY ANALYSIS USING GLM FRAMEWORK

Steps	Formulation
1. Model the CIF under GLM framework	$\log\lambda_i(t\|\theta_i,H(t)) = \theta_{i,0} + \sum_{n=1}^{N}\sum_{m=1}^{M_i}\theta_{i,n,m}R_{n,m}(t)$
2. Selecting the model order	Akaike Information Criterion
3. Likelihood of causality	$\Gamma_{ij} = \log\frac{L_i(\theta_i)}{L_i(\theta_i^j)}$
4. Determining directionality	$\text{sgn}\|\sum_{m=1}^{M_i}\theta_{i,j,m}\|$

milliseconds bins for the robotic control. Subsequently, the decoded outputs were translated into joint-space velocities.

III. CAUSALITY ANALYSIS

Temporal dynamics of individual neurons are often governed by other causally-connected neurons that are spatially distributed. To understand the connectivity within the ensemble of neurons, Granger causality-based technique has been used [13]. A point-process neural spike train can be characterized by its conditional intensity function (CIF), $\lambda(t|H(t))$, where $H(t)$ denotes the spiking history of all neurons in the ensemble up to time t. For a linear model implementation [14], the causality analysis comprises four essential steps (see Table-I).

Using a generalized linear model (GLM) framework, the log CIF was modeled as a linear combination of the covariates, $H(t)$, which describes the neural activity dependencies [15]. The logarithm of the CIF for neuron i is given as,

$$\log\lambda_i(t|\theta_i,H(t)) = \theta_{i,0} + \sum_{n=1}^{N}\sum_{m=1}^{M_i}\theta_{i,n,m}R_{n,m}(t), \qquad (1)$$

where $\theta_{i,0}$ relates to a background level of activity, and $\theta_{i,n,m}$ represents the effect of ensemble spiking history $R_{n,m}(t)$ of neuron n on the firing probability of neuron i at time t for $n = 1,...,N$ neurons. The model order, i.e., the history for each neuron needed for best approximation was identified using AIC (Akaike's information criterion). In this work, a history of maximum 60 milliseconds with a 3 milliseconds window was used.

To estimate the causality between two neurons, a log-likelihood ratio was proposed in [13]. Accordingly, it is given by,

$$\Gamma_{ij} = \log\frac{\Pr(\text{t}+1 \text{ of } i|\text{past of everyone till t})}{\Pr(\text{t}+1 \text{ of } i|\text{past of everyone except } j \text{ till t})} \qquad (2)$$

A Γ_{ij} of greater than zero represents a causal relationship between neurons i and j. The point process likelihood function for neuron i, $L_i(\theta_i)$ was estimated including all the covariates, and subsequently, the relative reduction in the likelihood $L_i(\theta_i^j)$ by excluding the history of neuron j was determined. Thus, the ratio between the two likelihoods is given by

$$\Gamma_{ij} = \log\frac{L_i(\theta_i)}{L_i(\theta_i^j)} \qquad (3)$$

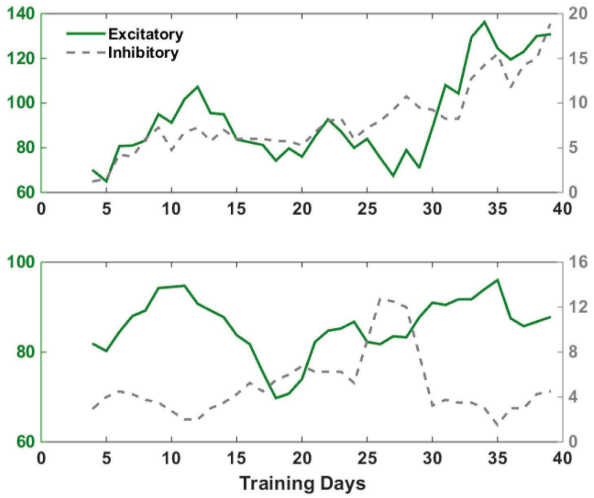

Fig. 1. Causal connections emerging in the ensemble as learning progressed is shown. (Top) shows the increase in the number of both excitatory and inhibitory connections within the reach cluster. (Bottom) shows the changes in role of the connectivity in the ensemble of grasp neurons.

If the spiking activity of neuron j has a causal influence on that of neuron i in the Granger sense, the likelihood $L_i(\theta_i)$ is greater than $L_i(\theta_i^j)$. Finally, the directionality, i.e., excitatory or inhibitory, was distinguished by the sign of $\sum_{m=1}^{M_i}\theta_{i,n,m}$, which represents the average causal influence.

The computational complexity of the entire GLM GC algorithm is of $\mathcal{O}(n^2)$. And, the top-level scheduling was handled in a Linux cluster using Swift. Implementation of the computational processes used a three-tier schema comprising of (i) a functional program layer, (ii) parallelizing scripts and (iii) wrapper start-up scripts for configuration and other parameterization. The functional programming was implemented in Matlab and the parallel script was created using Swift. The node-level parallelization was managed using Swift and the core-level management was implemented using parallelization tools from the shell and Matlab. And, the low-level algorithmic implementation was coded in Matlab using an adopted version of [13].

IV. RESULTS

Two independent clusters, i.e., 19 neurons for reach and 10 for grasp velocity control, were analyzed as a single ensemble, and spike trains extracted for behavioral epochs. Thresholds were applied to the z-Scored decoded velocities, and periods with 500 milliseconds of near-zero velocity followed by transitions that were larger than 1.2σ within a 50 milliseconds window and sustained for another 500 milliseconds were considered as epochs. Binned spike trains corresponding to the epochs were chosen for further analyses. The animal was trained over a period of 37 days and the number of excitatory and inhibitory connections that evolved during training is shown in Figure-1. As learning progressed, the number of neurons that were causally connected increased within the reach cluster. For the grasp cluster, though the

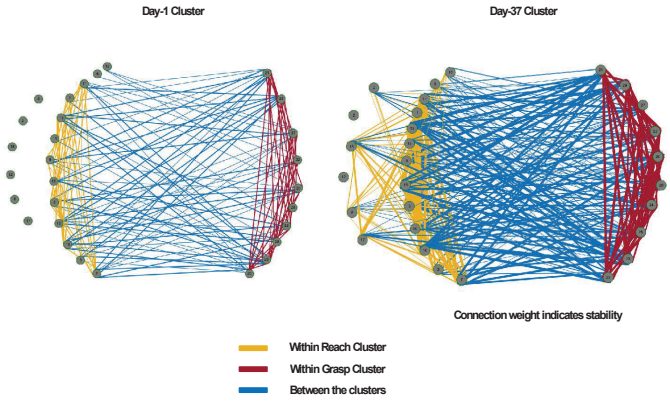

Fig. 2. Comparison of the ensemble connectivity between days 1 and 37. (Left) shows the network on Day-1, with 6 isolated neurons in the reach cluster. Later after training (right), 4 of the 6 neurons were recruited within the network. Also, the connection strength and stability between the two clusters increased consistently.

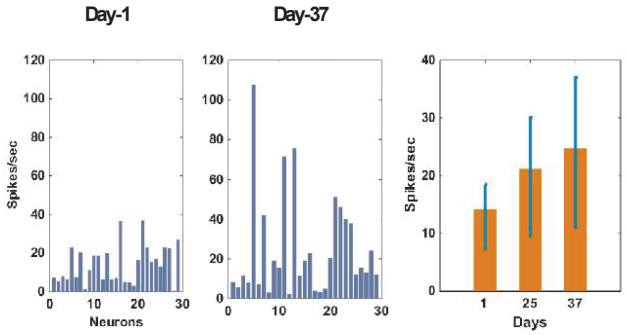

Fig. 3. Mean firing rate of the neurons show a longitudinal increase from day-1 to day-37. The relationship between the firing rate and the connectivity is not trivial.

increase in the number of connections was minimal, the affector role showed changes. The number of connections and the connection strengths increased within and between the clusters as learning progressed. Figure-2 shows the in and out-degree connections for the 29 neurons at the start and end of the training days. Changes in the mean firing rate of the neurons is shown in Figure-3).

Changes in the mean coherency between channels within the reach and grasp clusters and the rest of the channels is shown in Figure-4 for β and low-γ frequencies.

V. Discussions

Spatiotemporal dynamics of ensemble of neurons is an influencing factor in BMI performance. Neurons in the network are adaptive in terms of their spatial and temporal connectivity and exhibit changes in both short and long-term learning epochs. It is reasonable to assume that these changes enable generation of volitional control on the BMI.

In the present study, the animal was a chronic amputee for over 7 years, and the causal network gradually emerged in terms of increased number of in- and out-degree connections within the ensemble. The characteristics of the two clusters were different in terms of their baseline con-

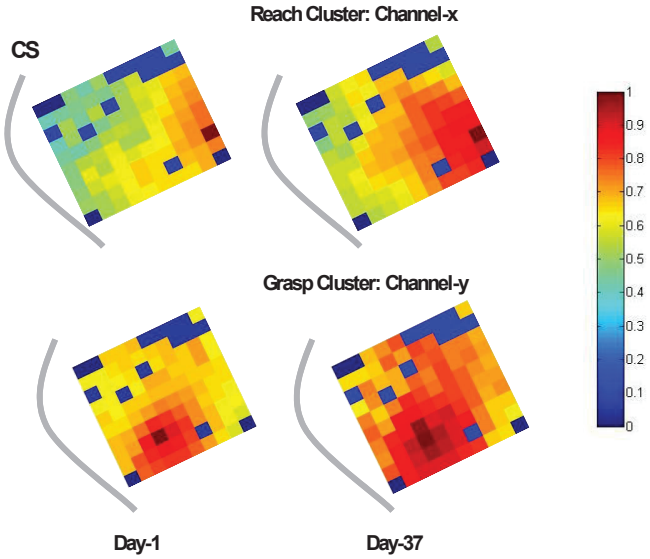

Fig. 4. Mean coherency between selected channels in the reach and grasp cluster paired with the remaining channels showed an increase in specific frequency bands. The change was prominent in the proximal regions of the selected channel.

nectivity. Channels in the reach cluster was chosen to be spatially in proximity to one another, while the grasp cluster was chosen to have functional correlation in their firing. Results show that the reach cluster had lesser number of functional connections in the initial stages of BMI learning and gradually increased significantly. On the other hand, neurons in the grasp cluster exhibited connectivity even in the early training days, i.e., they had near-saturation connectivity. With learning, the causal connectivity within the grasp neurons was limited by the upper bound of possible connections. However, the neurons showed changes in their role as excitatory or inhibitory connections, longitudinally.

The LFPs also showed increase in coherencies in specific frequency bands, i.e., in the β and the low-γ regions of the spectrum. The coherency changes originated in the proximity of the observed channels and radially propagated across the entire area of the array. While the genesis of LFPs and their input-output relationship with spike trains are debatable, it ie nevertheless observed here that both the modalities showed increase in their functional connectivity.

Reaching to grasp with an intact arm involves a typical coordinated velocity profile for the two components. In cases of BMIs, learning a synergistic reach and grasp is often preceded with a componentized execution strategy, i.e., the reach and grasp velocities are sequentially executed one inhibiting the other. This is a common phenomenon observed in infants learning to reach and grasp. Similar behavior can be inferred from the causal connections exhibited in the present study. The number of inhibitory connections between the two clusters increased such that the grasping behavior is inhibited till the robot reaches towards the object and when grasping occurs, the reaching is suppressed.

Network interactions can be studied at various temporal

scales, i.e., dynamics associated with state-space changes during task execution and those related to long-term learning. Here, we have shown the statistically inferred network emergence in a small region of M1 as BMI learning occurred.

ACKNOWLEDGMENT

KB, KT, and NGH would like to thank the staff at animal research center, University of Chicago. KB and NGH would like to thank Andrew Fagg and Joshua Southerland for their support with the robotic controller.

REFERENCES

[1] Eberhard E. Fetz, "Volitional control of neural activity: implications for brain-computer interfaces," *The Journal of Physiology*, vol. 579, no. 3, pp. 571–579, 2007.

[2] Brittany Mei Young, Zack Nigogosyan, Alexander Remsik, Léo M Walton, Jie Song, Veena A Nair, Scott W Grogan, Mitchell E Tyler, Dorothy Farrar Edwards, Kristin Caldera, et al., "Changes in functional connectivity correlate with behavioral gains in stroke patients after therapy using a brain-computer interface device," *Frontiers in neuroengineering*, vol. 7, 2014.

[3] AM Green, CE Chapman, JF Kalaska, and F Lepore, "Stimulus-driven changes in sensorimotor behavior and neuronal functional connectivity: application to brain–machine interfaces and neurorehabilitation," *Enhancing Performance for Action and Perception: Multisensory Integration, Neuroplasticity and Neuroprosthetics*, vol. 191, pp. 83, 2011.

[4] Ann-Shyn Chiang, Chih-Yung Lin, Chao-Chun Chuang, Hsiu-Ming Chang, Chang-Huain Hsieh, Chang-Wei Yeh, Chi-Tin Shih, Jian-Jheng Wu, Guo-Tzau Wang, Yung-Chang Chen, Cheng-Chi Wu, Guan-Yu Chen, Yu-Tai Ching, Ping-Chang Lee, Chih-Yang Lin, Hui-Hao Lin, Chia-Chou Wu, Hao-Wei Hsu, Yun-Ann Huang, Jing-Yi Chen, Hsin-Jung Chiang, Chun-Fang Lu, Ru-Fen Ni, Chao-Yuan Yeh, and Jenn-Kang Hwang, "Three-dimensional reconstruction of brain-wide wiring networks in drosophila at single-cell resolution," *Current Biology*, vol. 21, no. 1, pp. 1 – 11, 2011.

[5] Seung Wook Oh, Julie A Harris, Lydia Ng, Brent Winslow, Nicholas Cain, Stefan Mihalas, Quanxin Wang, Chris Lau, Leonard Kuan, Alex M Henry, et al., "A mesoscale connectome of the mouse brain," *Nature*, vol. 508, no. 7495, pp. 207–214, 2014.

[6] P Somogyi, AJ Hodgson, and AD Smith, "An approach to tracing neuron networks in the cerebral cortex and basal ganglia. combination of golgi staining, retrograde transport of horseradish peroxidase and anterograde degeneration of synaptic boutons in the same material," *Neuroscience*, vol. 4, no. 12, pp. 1805–1852, 1979.

[7] Amon T. Ferry, Dost ngr, Xinhai An, and Joseph L. Price, "Prefrontal cortical projections to the striatum in macaque monkeys: Evidence for an organization related to prefrontal networks," *The Journal of Comparative Neurology*, vol. 425, no. 3, pp. 447–470, 2000.

[8] FG Wouterlood and HJ Groenewegen, "Neuroanatomical tracing by use of phaseolus vulgaris-leucoagglutinin (pha-l): electron microscopy of pha-l-filled neuronal somata, dendrites, axons and axon terminals," *Brain research*, vol. 326, no. 1, pp. 188–191, 1985.

[9] Jacopo Annese, "The importance of combining mri and large-scale digital histology in neuroimaging studies of brain connectivity," *Mapping the connectome: Multi-level analysis of brain connectivity*, 2012.

[10] Karthikeyan Balasubramanian, Joshua Southerland, Mukta Vaidya, Kai Qian, Ahmed Eleryan, Andrew H Fagg, Marc Sluzky, Karim Oweiss, and Nicholas Hatsopoulos, "Operant conditioning of a multiple degree-of-freedom brain-machine interface in a primate model of amputation," in *Engineering in Medicine and Biology Society (EMBC), 2013 35th Annual International Conference of the IEEE*. IEEE, 2013, pp. 303–306.

[11] Seif Eldawlatly, Rong Jin, and Karim G Oweiss, "Identifying functional connectivity in large-scale neural ensemble recordings: a multiscale data mining approach," *Neural computation*, vol. 21, no. 2, pp. 450–477, 2009.

[12] I. Badreldin, J. Southerland, M. Vaidya, A. Eleryan, K. Balasubramanian, A. Fagg, N. Hatsopoulos, and K. Oweiss, "Unsupervised decoder initialization for brain-machine interfaces using neural state space dynamics," in *Neural Engineering (NER), 2013 6th International IEEE/EMBS Conference on*, Nov 2013, pp. 997–1000.

[13] Sanggyun Kim, David Putrino, Soumya Ghosh, and Emery N. Brown, "A granger causality measure for point process models of ensemble neural spiking activity," *PLoS Comput Biol*, vol. 7, no. 3, pp. e1001110, 03 2011.

[14] K. Takahashi, L. Pesce, J. Iriarte-Diaz, Sanggyun Kim, T.P. Coleman, N.G. Hatsopoulos, and C.F. Ross, "Granger causality analysis of functional connectivity of spiking neurons in orofacial motor cortex during chewing and swallowing," in *Engineering in Medicine and Biology Society (EMBC), 2012 Annual International Conference of the IEEE*, Aug 2012, pp. 4587–4590.

[15] Wilson Truccolo, Uri T Eden, Matthew R Fellows, John P Donoghue, and Emery N Brown, "A point process framework for relating neural spiking activity to spiking history, neural ensemble, and extrinsic covariate effects," *Journal of neurophysiology*, vol. 93, no. 2, pp. 1074–1089, 2005.